Science
AAAS

Supplementary Materials for

Evolutionarily conserved role of oxytocin in social fear contagion in zebrafish

Ibukun Akinrinade *et al*.

Corresponding author: Rui F. Oliveira, ruiol@ispa.pt

Science **379**, 1232 (2023)
DOI: 10.1126/science.abq5158

The PDF file includes:

Other Supplementary Material for this manuscript includes the following:

Materials and Methods

The experimental procedures described herein follow recommendations detailed in the ARRIVE (Animal Research: Reporting of *In Vivo* Experiments) "Essential 10" checklist [31]. The checklist details the necessary components for assessing the reliability of reported animal research, including: (1) study design in terms of identifying experimental units and control groups; (2) reporting sample sizes, which we specify in our figures, and how these were determined, which we explain below; (3) exclusion criteria, which we adopted at specific steps; (4) randomization procedures for allocating animals in treatment groups , which we used together with counterbalancing to control for biases; (5) blind quantification, which was ensured by our use of automated computerized tracking of behavior; (6) description of outcome measures, which we provide for every experimental procedure together with any calculations used to quantify variables used in analysis; (7) statistical methods, which we provide in detail together with criteria for their choice based on their assumptions and if these were met; (8) characterization of experimental animals, which we do by specifying species, strain/line, genotype, sex and age; (9) experimental procedures, which we describe in terms of set-up, experimental manipulation, timing, sequential organization and the adoption of appropriate acclimation periods; (10) results, where we include descriptive statistics and effect sizes.

Animals, housing, and husbandry

We used naïve adult zebrafish, *Danio rerio,* in all experimental procedures, with the number of animals used in behavioural tests kept at ≥ 12, which is necessary for statistical significance at higher effect sizes and powered for detecting reasonable, biologically relevant, effects at low error probability [32, 33]. Wild-type (WT) male fish of the *TU* strain, aged 6 - 12 months, were used to characterize the expression of oxytocin receptors. Transgenic male fish from a mixed *TL* background, aged 3 - 6 months, included the *oxt*:EGFP line, for characterizing oxytocin fibre projections, and the double reporter line *vglut2a:*dsred*/gad1b:*GFP, for characterizing glutamatergic and GABAergic activity. The three genetically modified (GM) lines used to target the oxytocin system, with mutation in either the *oxt* (ligand), *oxtr* or *oxtrl* (receptors) gene, and their respective WT controls, were also of a mixed *TL* background, and used in all other experimental procedures. For the video playbacks experiment, used to test attention, contagion and distressed-state recognition, fish were aged 6 - 9 months and were of both sexes: 65 *oxt* mutant fish (base: 18M, 7F; oxytocin injection: 10M, 10F; vehicle injection:11F, 9M) and 65 WT as a control (base: 25M; oxytocin injection: 4M, 8F; vehicle injection: 9F, 3M); 25 *oxtr* mutant fish (17M, 8F) and 25 WT as a control (20M, 5F); 26 *oxtrl* transgenic fish (males) and 25 WT as a control (males). All other experiments with these strains included only males aged 3 - 6 months.

All fish were housed in groups at a density of 10/L in a recirculation life support system (Tecniplast) maintained at 28 °C, pH 7.0, conductivity 1000 μS/cm and 14 L:10D photoperiod. Feeding included a combination of live (*Paramecium caudatum* and *Artemia salina)* and dry food

(Gemma). Husbandry, health maintenance and welfare protocols were followed as previously described [34], and fish were kept free from known pathogens via sentinel testing. All experiments were conducted in accordance with standard operating procedures of the Institutional Ethics Committee, assessed and monitored by the Animal Welfare Body, and licensed by the National Competent Authority (DGAV-Direcção Geral de Alimentação e Veterinária, Portugal) with the permit number 0421/000/000/2020.

Genetic line characterization: modification of oxytocin signaling

The *oxt* mutant line (ZFIN ID: ZDB-ALT-180904-7) is a functionally null line with a small deletion of 7 base pairs in Exon 2 following treatment with CRISPR1-oxt at the embryonic stage, described by Blechman et al. [35]. It is a frameshift mutation leading to disruption of the translational reading and abolishing the expression of the oxytocin neuropeptide, and thus overall oxytocin signaling. The *oxtr* mutant line (ZFIN ID: ZDB-ALT-190830–1) is a functionally null mutant line that has a small deletion of 1 base pair following treatment with TALEN1-oxtr at the embryonic stage. It is a frameshift mutation that abolishes the expression of oxytocin receptor 1. The characterization of the line has been further described by Nunes et al. [36]. The *oxtrl* transgenic line (ZFIN ID: ZDB-ALT-190819-1) has an insertion of a multi-frame stop cassette (83bp) at the ATG+260 position leading to a stop codon formation after the 89th amino acid, following CRISPR treatment at the embryonic stage, which abolishes the expression of the oxytocin receptor 2. Finally, the *oxt:EGFP* transgenic reporter line (ZFIN ID: ZDB-ALT-111103-1) was generated using the Tol2kit transposon-based vector system for encoding the *oxt* gene and report the endogenous expression of *oxt* mRNA and protein [35]. All genetic lines were generated at the Weizmann Institute of Science, Israel, by G. Levkowitz, and in collaboration with R. Nunes for the *oxtr* transgenic line and M. Gliksberg for the *oxtrl* line.

Genotyping

Genotyping was performed by PCR of the genomic region of interest from clipped fins, followed by sequencing [36]. We designed specific primer pairs to target the deletion sites of the ligand [*oxt* (NM_178291.2): 5` – AGACACAAACACTAAGTAA – 3` (forward), 5` – AGCAGACGGACAGCAGACACAGCA – 3` (reverse)] and receptors [*oxtr* (NM_001199370.1): 5‘ – TGCGCGAGGAAAACTAGTT – 3‘ (forward), 5‘ – AGCAGACACTCAGAATGGTCA – 3‘ (reverse); *oxtrl* (NM_001199369.1): 5‘ – TTTTACGCACAATGGAGAGCC – 3‘ (forward), 5` – AGCATGTAAGTGGACGCGAA – 3’ (reverse)].

Alarm substance extraction

Alarm substance was extracted by following approved procedures under institutional and project licenses. Briefly, 12 adult fish of either sex (to control for variations) were euthanised via rapid chilling, placed on a petri dish kept on ice and 15 superficial surgical-blade cuts were performed on either side of their trunk to induce the release of alarm substance from the club cells. Cuts were then washed with 50ml of distilled water and filtered with a 240mm filter paper (VWR

cat no. 516-0287) to remove impurities. The extracted solution from all fish was mixed and stored in individual aliquots of 0.75 ml in -20^{o}C.

Oxytocin treatment

To test the reversal of effects from non-functioning oxytocin signalling, *oxt* KO and WT controls were treated with either the fish homologue of oxytocin (isotocin; *Ser4*, *Ile8*-Oxytocin; Cat. No. 4030890.0005, Bachem, Germany) or vehicle controls. For the treatment, first were anaesthetised by immersion in MS-222 solution (100mg/L), weighted and placed with their ventral part exposed in a pre-cut fissure on a foam bed saturated in water. Fish were then administered a 2 µl/g (μ weight = 2.5g ± 0.8) intraperitoneal injection (30G needle) of either saline (vehicle control) or isotocin solution in saline (0.9%) at 1ng/kg, based on dose-response tests by Braida et al. [37]. The administration period was ~20s, after which fish were placed in a small compartment with tank water and allowed 2 min to recover with the help of oxygen supply from air bubbles slowly pipetted near their gills.

Behavioral test for social transmission of fear

Focal fish were randomly assigned to either of three conditions: to observe a shoal exposed to the alarm substance, to observe a shoal exposed to distilled water (vehicle control) or to be exposed to the alarm substance directly without observing any demonstrators (control for social transmission). The order of testing was randomized for each individual and conducted between 10:00 and 19:00. Animals were removed from home tanks on the day before experiments, randomly assigned to treatment groups, and kept in their experimental tank overnight for acclimatization. Experimental tanks had visual access to identical adjacent tanks (1.3 L; 12 × 12 × 15 cm) but were visually isolated from other external cues via opaque covers. Adjacent tanks kept either an unfamiliar shoal of two males and two females (Fig. 1A) or remained empty for the social transmission control. Each trial lasted for 15 min, including a 5 min baseline period followed by a 10 min post-exposure period. The alarm substance was kept on ice to avoid degradation during the trials and, thus, distilled water for the vehicle control was kept in the same conditions. Substances were administered via a flexible and transparent PVC tubing (diameter: 0.8 mm internal, 2.4 mm external).

Behavioral test of fear recognition

This test used video playbacks, which enabled us to control for inter-individual variation in demonstrators by presenting focal fish videos of the same fish in two separate states, neutral and fearful. The ability of fish to perceive and respond to videos of conspecifics under identical conditions, was demonstrated by Nunes et al. [36], which provide a detailed analysis of response to features of biological motion. Demonstrators used in video playbacks were recorded with a goPro camera (goPro hero3+, 60 fps, 1080 pixel resolution) placed in front of a 1.5 L tank, behind an opaque acrylic sheet with a customised cut-out for the camera lens, to keep the investigator covered during manipulations. The rest of the tank walls kept covered to reduce further visual

interference and contained a flexible and transparent PVC tubing for substance administration (diameter: 0.8 mm internal, 2.4 mm external). A 10 minute recording of the tank was first captured to be used during the acclimatisation phase of experiments. Each fish used as a demonstrator was kept in the tank overnight, with the camera in place, and the following morning was recorded. During recording, following a 200s capture of baseline behaviour, the investigator released 0.75 ml (per 1.3L of water) of alarm substance and recorded for a further 200s, to capture erratic movement and freezing behaviour. Videos were edited using the VSDC© software (v. 6.3.6.18; Flash-Integro LLC, 2019) and included: a 10 min video of the housing tank of demonstrators used as *background video* during acclimation; a 5 min *control video* with the demonstrator swimming (neutral state), which included 3 repetitions of a 100s swimming period; a 5 min *stimulus video* with the demonstrator periodically exhibiting fear, which included 3 repetitions of a 60s swimming period followed by 40s bout of an erratic and freezing repertoire. During tests, videos were displayed on monitors as real size images.

Experiments were carried out in a 4.5 L test tank (29.5 × 14.5 × 11 cm), stationed on a light box with infrared LEDs and with two LCD monitors (Asus VG248, 1080 HD, 144 Hz rapid refresh rate) positioned on either side, remaining visible through the glass walls **(**Fig. 4A**)**. The rest of the tank was covered with opaque lining and the overall set-up was housed in a compartment covered with a light-blocking black fabric to prevent visual interference from external stimuli. Playback screens were controlled and synchronised via a third screen connected to the same computer (TightVNC remote control software). Focal fish were kept in overnight isolation, housed individually in opaque tanks (12 × 12 × 15 cm) at 28 °C and a 14 L: 10 D photoperiod. The following day fish were individually placed in a central compartment of the test tank, devised by two removable transparent partitions, and acclimatized for 10m to the background video projected by both LCD screens. Following acclimation, one monitor was set to play the 5 min control video (neutral state) and the other the stimulus video (periodic fearful state), with the side of the video and the identity of the demonstrator (1 male and 1 female) counterbalanced across subjects. Following this stage, the partitions were lifted and fish allowed access to the entire tank for 10 min while playbacks on both sides displayed the control video (played twice in sequence). Focal fish were unfamiliar (i.e. have had no previous contact) with the videoed demonstrators.

Data extraction

For each test a continuous video-recording was obtained, using a high definition camera for the fear transmission test (Logitech B 525; acquisition at 30 fps) and a black-and-white camera with infrared sensitivity (Henelec 300B; acquisition at 30 fps) for the fear recognition test. The shift to the infra-red recording in the second test facilitated automated tracking over the larger arena, using the infra-red light backdrop from experimental set-up (Fig. 4A). Videos were fed to a remote laptop computer using the recording software Pinnacle Studio (v. 12, http://www.pinnaclesys.com). Individual recordings were then analyzed using the commercially available video tracking software Ethovision XT© 11.0 (Noldus Inc., The Netherlands), which provides automated observer-free measures from the videos.

For the fear transmission tests, recordings of the whole tank were tracked over the 15 min trial period to extract measures used to quantify fear behavior, both for the 5 min baseline period and the 10 min post-exposure period. These included proportion time spent exhibiting erratic movement [acceleration > 8 cm/s^2 and > 5 changes in direction/sec (> 90°)] and freezing (velocity < 0.2 cm/s).

For the fear recognition tests two separate stages were scored. First, for the first 5 min period of video observation, the zone of the central compartment in which animals were restricted was set as a region of interest (ROI) and animals tracked within this region. Attention to video playbacks was measured by the absolute compass heading (*x* direction relative to the stimulus video, ranging from 0° to 180°). Fear transmission was again measured by proportion time in erratic movement and freezing, and validated by added kinematic quantifiers [angular velocity (turn angle per frame); speed (cm/s)], and matched to the same measures extracted from the playback videos for validating transmission. Second, for the final 10 min of the test, during which full-tank access was allowed, the compartments next to each video were set as ROIs (Fig. 4A) and 3 measures were extracted: total distance travelled (exploration); latency time to first entry at either ROI (approach motivation); and the total time spend within each ROI (local preference).

Quantification of neuronal activation using the neuronal activation marker phospho-S6 ribosomal protein (pS6)

Brain tissue was collected for the quantification of brain activation and functional connectivity in *oxtr* experimental fish (mutants and WT controls) following the social transmission of fear experiment (1 hr post testing). Animals were anaesthetized with ice-cold water and their head extracted by cervical transection, fixed in 10% formalin for 3 days (in room temperature; RT), rinsed twice in 1× PBS (30min) and kept in EDTA (0.5 M, pH=8) for a further 2 days (RT). Coronal sections (5µm) of samples were extracted for immunohistochemical staining and microscopy, following paraffin-embedding.

Sectioned brains were stained for the pS6. Slides were first kept in Tris-EDTA at 95°C (20 min) for antigen retrieval. Non-specific binding was blocked by a 1 hr in 1% BSA TBS incubation (0.025% Triton X-100) at RT and an overnight incubation in the primary antibody prepared in blocking solution (pS6 Ser$^{235/236}$ antibody D57.2.2E Rabbit mAB #4858 1:400; at 4 °C. Slides were then rinsed in TBS (0.025% Triton X-100) and incubated in the secondary antibody prepared in blocking solution (Alexa 594- Invitrogen goat anti-rabbit # A-11037 1:1000, Alexa 488- Invitrogen goat anti-chicken A-11039 1:1000). Slides were then washed in TBS with and then without 0.025% Triton X-100, before 20 min incubation in DAPI (4',6-diamidino-2-phenylindole) for nuclei counterstaining and rinsed in TBS before mounting (Biotium, Everbrite- 23003).

pS6 positive cells quantification projections visualization was performed on 20-fold magnified sections (Zeiss Axioscan.Z1 slide scanner) and analyzed via the Zeiss Zen blue 2.1 imaging software. Five consecutive coronal sections were quantified for each brain region (Fig. S6), where positive pS6 cells were counted in 1000 µm quadrants.

Quantification of active inhibitory (GABA) and excitatory (glutamte) cells

To quantify excitatory and inhibitory activity in experimental fish of the double reporter line *vglut2a:*dsred / *gad1b:*GFP, following the social transmission of fear experiment (1 hr post testing), we used immunostaining with pS6 and DAPI to identify active cells, and with GFP and dsRed antibodies to quantify GABA (*gad1b*) and glutamate (*vglut2a*) sites, respectively.

On day one of the immunostaining protocol, slides were deparaffinized and exposed to antigen with Tris-EDTA (10mM TrisBase, 1mMEDTA) 0.05% Tween 20, pH 9.0. Samples were then incubated in Tris-EDTA at 95°C for 20 min, removed and left to chill without the lid for 15 min, washed three times in TBS 0.025% Triton X-100 with gentle shaking for 10 min, and blocked by incubation with TBS 0.025% Triton X-100 + 1% BSA (albumin) for 1 hr at room temperature. The samples were finally incubated with the primary antibody [anti-pS6 (mouse; 1:400), anti-GFP (chicken; 1:200), anti-dsRed (rabbit; 1:200)] in TBS 0.025% Triton X-100 + 1% BSA overnight at 4°C in humid chamber.

On day two, samples were first washed in TBS 0.025% Triton X-100 (3 times for10min) by gentle shaking and incubated with the secondary antibody (1:500; anti-mouse 647, anti-chicken 488, anti-rabbit 568) in TBS 0.025% Triton X-100 + 1% BSA for 2 hr at room temperature. Samples were then washed in TBS 0.025 Triton X-100 (twice for 10 min) by gentle shaking and finally incubated in DAPI (1:500 in TBS) for 20 min at room temperature, before mounting slices with EverBrite Hardset medium.

Stained brain sections were acquired at 20-fold magification using the Zeiss Imager Z2 + ApoTome.2 slide scanner and analyzed using the ImageJ Java software. Slices were counted alternately so that cells were not considered in duplicate. In each region, we identified DAPI stained cells with the pS6 signal and counted the total as well as those overlapping with either the GFP (GABA; *gad1b*) or dsRed (glutamate; *vglut2a*) signals. Co-localizations of pS6 positive cells with either GFP or dsRed were measured in % active cells such that:

$$\%\,\text{active} = \left(\frac{no.\ colocalized\ with\ pS6}{total\ no.}\right) \times 100$$

Imaging of oxytocin projections

OXT:GFP (Tg(*oxt*:EGFP)wz01 ID: ZDB-ALT-111103–1) positive fish were euthanized in Tricaine, and their heads and skull removed. the heads were then fixed O.N at 4C in 4% PFA on a shaker. After fixation the brains were removed from the skull and subjected to whole-mount immunohistochemistry as per standard protocol: PFA was washed out, and samples were placed in ice cold (-20C) acetone in a freezer at -20C for 10 minutes. The acetone was washed out, and the samples were then incubated in blocking solution (PBS + 0.1% triton, 1% DMSO, 1% BSA, 5% NGS) for minimum of 2 hours at R.T and then incubated with primary Ab diluted at 1:200 ((anti-TH, Mouse monoclonal anti-Tyrosine hydroxylase, Merck-millipore, CAT: #MAB318) and anti-GFP (Chicken polyclonal anti-GFP IgY Antibody Fraction, Life Technologies, CAT: #A10262)) O.N at 4C on the shaker. The following morning, Samples were washed

repeatedly (minimum of 6X15 minute washes) with blocking solution and then placed in blocking solution containing fluorescent secondary antibody at 1:200 O.N at 4C on a shaker. The following morning, Brains were submerged in 4% Noble Agarose, allowed to cool at 4C, and then sliced in a vibratome in ice-cold PBS at a thickness of 200 um. Slices were then mounted on a slide in mounting medium (Aqua-Polymount, polysciences, inc. 400 valley road, Warrington PA 18976, CAT: 18606-20) and imaged on a Zeis LSM 800 scanning confocal microscope.

Expression of oxytocin receptors in the brain

Brain tissue was also collected for testing the expression of oxytocin receptors (oxtr and oxtrl) in WT fish. WT fish samples were embedded in cryomoulds (OCT Compound, Tissue-Tek, Sakura 4583) and cryosectioned (150 µm coronal, Leica CM 3050S cryostat) for microdissection.

Receptor expression in WT fish was tested following microdissection of target brain areas from the cryosections, collected under stereoscope (Zeiss Stemi 2000) with a modified 210 µm needle (1 per region to prevent cross-contamination). Target areas were selected based on their involvement in social regulation and decision making [15] and included: the olfactory bulb (Ob), the medial zone of the dorsal telencephalic area (Dm, putative homologue of the mammalian basolateral amygdala), the preoptic area (POA), and the ventral nucleus of the ventral telencephalic area (Vv, putative homologue of the mammalian lateral septum), the dorsal nucleus of the ventral telencephalic area (Vd, putative homologue of the mammalian striatum), the supracommissural nucleus of the ventral telencephalic area (Vs, putative homologue of the mammalian medial extended amygdala and the bed nucleus of the stria terminalis), and the postcommissural nucleus of ventral telencephalic area (Vp). The Ob, Vv, Vd, Vs/Vp (pooled due to proximity), and POA were collected from both hemispheres at a single sampling point, due to their small size when compared to the diameter of the microdissection. The Dm was sampled from both hemispheres separately, and tissue was then pooled directly into lysis buffer and stored at -80°C until mRNA extraction.

For RNA extraction tissue was homogenized in 100 μl of qiazol (lysis buffer) and incubated for 7 min at RT. 50 μl of Chloroform was then added and shaken vigorously for 15 s and the sample left to incubate at RT for 5 min. Samples were then centrifuged at 13000 g for 20 min at 4ºC, and the upper aqueous phase transferred to a new tube where 1 volume of 70% ethanol was added. This mixture was transferred to an RNEasy® column and left to stand for 5 min at RT, and then was centrifuged for 1 min at 9000 g. A series of buffers from the RNeasy® Lipid Tissue Mini Kit (Qiagen, 74804) were added to samples sequentially (700 μl of Buffer RW1, 500 μl of Buffer RPE and an additional 500 μl Buffer RPE), after each of which samples were centrifuged for 1 min at 9000 g and the flow-through discarded. The RNeasy column was then centrifuged a new 2 ml tube for 3 min at 14000 g and transferred to a separate new 1.5 ml tube where RNA was eluted with 25 μl of RNAse-free water, and centrifuged for 2 min at 9000 g. The elution step was repeated with the same RNAse-free water to increase RNA recovery efficiency and RNA screened

for concentration, purity (260 nm and 280nm spectrophotometric absorbance; Thermo Scientific NanoDrop 2000) and integrity (Agilent 2100 Bioanalyzer).

Pooled RNA of each brain area was reverse transcribed to cDNA (iScript cDNA Synthesis Kit, Biorad, 1708890) following the manufacturer's instructions. Briefly, in a clean Eppendorf tube, nuclease-free water, 5x iScript reaction mix (4μl), iScript reverse transcriptase (1μl), and RNA template (100 fg to 1 μg total RNA) were added up to a total volume of 20 μl and incubated in a PCR thermocycler (5 min priming at 25°C, 60 min reverse transcription at 42°C, 5 mins reverse transcription inactivation at 85°C, and kept at 4°C). Samples were subsequently stored in -20°C until use.

Diluted cDNA samples (1:10) were used as templates for quantitative polymerase chain reactions (qRT-PCR). Primer sequences for the oxytocin receptor (*oxtr*) and the reference gene (*eef1a1l1*: eukaryotic translation elongation factor 1 alpha 1, like 1) were designed in the Primer 3 software (Premier Biosoft International, Palo Alto, CA, USA) and primer sequences for oxytocin receptor-like (*oxtrl*) were provided by Gil Levkowitz. qRT-PCR reactions were performed in the Applied Biosystems quantstudio 7 thermocycler (7900 HT, Thermofisher) in 8 μl triplicate reactions with SYBR Green PCR Master Mix (Applied Biosystems, Thermofisher) with 50 µM primers for *oxtr* and *eef1a*, and 13.3 µM for *oxtrl* (Table S2). Thermocycling conditions were 5 min at 95°C, followed by 40 cycles of 95°C for 30 s, annealing temperature 60°C and62 ºC for 30 s, and extension at 72°C for 30 s (see Table S2 for details). After PCR, a melting curve program from 55 to 95°C with 0.5°C changes was applied and fluorescence cycle thresholds (*Ct*) were automatically measured.

Analysis

Statistical analyses, calculations and graphical representations were carried out using the software Graphpad Prism® (v. 8.0.1; GraphPad LLC, San Diego, CA), R© (v. 4.0.3; R Core Team) and Minitab® (v.17; Minitab Inc., State College, PA). Figures were edited and completed with illustrations using the software Adobe® Illustrator® (CS6, v.16.0.0; Adobe Systems Inc.) and Inkscape© (v. 0.92.4; Free Software Foundation Inc.). Continuous data were tested for normality using the Ryan-Joiner and Kolmogorov-Smirnov tests and homogeneity of variance was tested using the Bonnett's and Levene's tests. Finite ranging and proportion based scores were tested for normality using the D'Agostino & Pearson test (K^2), which confirms Gaussian distribution via skewness and kurtosis [38].

Genetic expression of receptor genes was calculated using the $2^{-\Delta Ct}$ method [39]:

$$2^{-\Delta Ct} = 2^{Ct_{Ref} - Ct_{Target}}$$

where Ct_{Ref} is the cycle threshold for the reference gene and Ct_{Target} is the cycle threshold for the target gene. Therefore, target gene expression was represented as relatively to the reference gene and quantified by the mean of this value across three technical replicates.

Cell counts of pS6 positive cells were tested via a generalized linear model with quasi-Poisson regression, with treatment (alarm substance or control) and genotype as fixed factors. A backward stepwise procedure was used to exclude non-significant effects, followed by *post-hoc* comparisons corrected with the two-stage linear step-up procedure for FDR-adjusted p-values.

Counts of GFP and dsRed positive sites with pS6 positive cells were tested via a generalized linear regression model with a log-link function, with treatment (alarm substance or control) as a fixed factor, and the total number of pS6 positive cells as a random covariate to control for individual differences from overall activity.

Percentage time erratic and freezing were compared between treatment groups using unpaired *t*-tests for parametric data, Welch's 2-sample *t*-tests for non-homogeneous normal data, and Mann-Whitney *U* tests for non-parametric data. Comparisons between lines were carried out using ANOVA tests, either at the two-way with treatment (alarm or control), or at the three-way when examining added effects from oxytocin injection (versus control) for testing recovery. Data not conforming to parametric assumptions were log-transformed $[log_{10}(x+1)]$. *Post-hoc* comparisons for testing differences between the treatments were corrected with False Discovery Rate (FDR) and *p*-value adjusted (Benjamini and Hochberg's method). Because of the large the time window (9 hrs) during which testing was carried out, we tested for putative circadian effects in our target behaviors. Given that no effects of time of day were found (Fig we have not included this para meter in subsequent analyses.

Compass orientation (absolute heading in degrees) was tested for differences from 90˚ by 1-sample *t*-tests to compare deviations from divided attention (see Fig. 2A) and compared between groups using Welch's 2-sample *t*-tests (due to unequal sample sizes).

Angular velocity and speed for each individual was measure by mean values from across the 3 replicates during observation, for both the 40s stress demonstration period and separately for the immediately preceding 40s under control conditions (neutral, swimming), in 10s time bins. For each of the two periods, stress and neutral control demonstration, we calculated the total area under the curve (AUC) across time bins using the trapezoid approximation method:

$$AUC_{t_{1-t_2}} = \frac{(x_1+x_2)}{2} \times (t_1 - t_2)$$

Behavioural change between states was then calculated as the difference in AUC between the control and stress demonstration periods (Δ AUC), for both speed and angular velocity. These values of change were tested for significant deviation from no difference ($\mu \neq 0$) by 1-sample *t*-tests and compared between groups using Welch's 2-sample *t*-tests (due to unequal sample sizes). To examine the degree of stress contagion, we tested consistency between observer and

demonstrator angular velocity and speed using a linear regression model with time bin as an interaction term for time-dependent changes.

Total distance travelled (cm) was compared between genotypes for all lines by Welch's 2-sample *t*-tests. To test for the effect of injections we used a two-way ANOVA with treatment (oxytocin or vehicle injection) and its interaction with genotype (WT or *oxt* KO) as predictors, and *post hoc* comparisons using Fisher's LSD.

Approach latency (s) towards the stimulus video ROI, where the demonstrator periodically stressed during observation, was compared to the approach latency towards the control-video ROI by Welch's 2-sample *t*-tests on the mean (due to unequal sample sizes) and effect sizes calculated using Cohen's *d* and the proportion of mean change, for each group. To assess the reversal of effects following injection treatments, for both the oxytocin and the vehicle treatment, we compared the directional effect size between WT and *oxt* KO. To do this we first calculated the sampling variance of each group:

$$v = \frac{1}{n_1} + \frac{1}{n_2} + \frac{d^2}{2(n_1 + n_2)}$$

and used this to compare Cohen's *d* values between genotypes, using a two-tailed *z*-test [40]:

$$z = \frac{d_1 - d_2}{\sqrt{v_1 - v_2}}$$

where, assuming normal distributions and known variances, the null hypothesis ($H_0 : d_1 = d_2$) can be rejected if $|z| \geq \pm 1.96$ at $\alpha = 0.025$ per tail (two-sided: $\alpha = 0.05$) [41].

Preference scores (PS) were calculated based on the time spend in ROI near the stimulus (ROI_S) and the control video (ROI_C) using:

$$PS = \frac{(ROI_S - ROI_C)}{(ROI_S + ROI_C)}$$

where values range between -1 (full preference for control) and 1 (full preference for stimulus). To validate that preference levels were statistically different from chance, we first tested if mean preference scores for each group were significantly greater or lower than 0, depending on the direction, by using 1-sample *t*-tests. Comparisons of preference scores between WT and KO fish for each line were performed using Welch's 2-sample *t*-tests (due to unequal sample sizes). To test for the effect of injections we used a two-way ANOVA with treatment (oxytocin or vehicle injection) and its interaction with genotype as predictors, and *post hoc* comparisons using Fisher's LSD.

For brain connectivity analysis, networks representing the co-activation patterns for each treatment were constructed as follows. For the case of M specimens, characterized by one sample (cell count) reading x_i for each of the N brain regions, the M-dimensional vector $\mathbf{x}_i$ was considered,

where *i* labels the region, and then computes the correlations c_{ij} for all region pairs, obtaining a weighted correlation matrix that we interpret as the adjacency matrix of a functional network. We then filtered each layer using the networks for each treatment as described by De Vico Fallani et al. [42] keeping the links with larger weight (in absolute value) up to a threshold density of $\rho = 0.17$. For the analysis of the excitation and inhibition patterns, we separate the weighted and signed graph in two subgraphs containing respectively only the positive and negative links, which we interpret as pertaining to network excitation and inhibition configurations. Distributions were compared by the two-sample Kolmogorov-*Smirnov test* and averages using the Mann-Whitney *U* test.

For the ranking of node strengths and correlations we compared, for all treatments, the strength (weighted degree of the full correlation matrix) of nodes in the standard way and rank them in descending order. To assess, similarities between ranking corresponding to different treatments, Kendall-Tau rank correlations were used and only correlations with $p<0.01$ were retained as significantly different from zero.

For the Detection of communities and extraction of preserved submodules we used the spin glass community detection method [43] applied on the average treatment network, obtained by averaging over the corresponding graph tower matrices. To increase the robustness of the detection, for each treatment, we repeated the community detection 1000 times. We computed the (center) consensus partition for each treatment from the 1000 candidate partitions, extracted as described by Peixoto [44].

To identify parts of modules that are shared between communities in different treatments, we study the distribution of intersection sizes. In particular, for two partitions we consider partitions $P_y = \{C_y^0, C_x^1, \ldots . . C_x^m\}$ and $P_y = \{C_y^0, C_y^1, \ldots . . C_y^l\}$ for treatments x and y, and then compare for each pair of modules (C_x^i, C_y^j) the intersection $J_{x,y}^{i,j} = C_x^i \cap C_y^j$ and then measure its cardinality$|J_{x,y}^{i,j}|$. We compute the significance of the measured intersection sizes by a permutation test based on a null distribution $p_0(|J|)$ constructed as follows: for a pair (C_x^i, C_y^j), we sample uniformly at random 10000 pairs of node sets with cardinality respectively $|C_x^i|$ and $|C_y^j|$and compute the size $|J|$ of their intersection. We consider statistically significant and thus retain the observed submodules $J_{x,y}^{i,j}$ such that $|J_{x,y}^{i,j}| > \mu(|J|) + 3\sigma(|J|)$ (equivalent to a $p < 0.01$ significance threshold), where $\mu(|J|)$ and $\sigma(|J|)$ are the first two moments of $p_0(|J|)$.

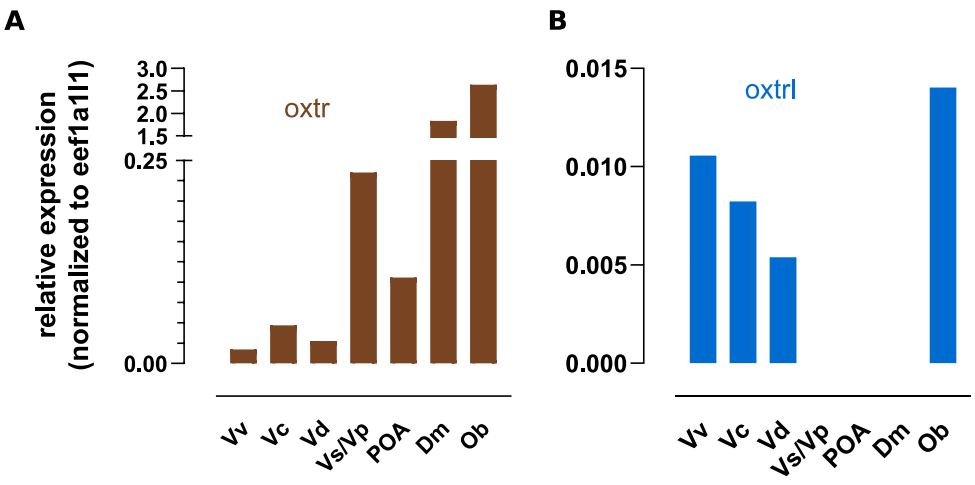

Fig. S1.

Relative expression of the two oxytocin receptors in areas of the social decision-making network in the zebrafish forebrain. (A) The main receptor (*oxtr*) was expressed in all areas of the network and in greater levels than (B) the second receptor (*oxtrl*), which was limited in the olfactory bulb (Ob) and the central, ventral and dorsal nucleus of the ventral telencephalon (Vc, Vv, Vd).

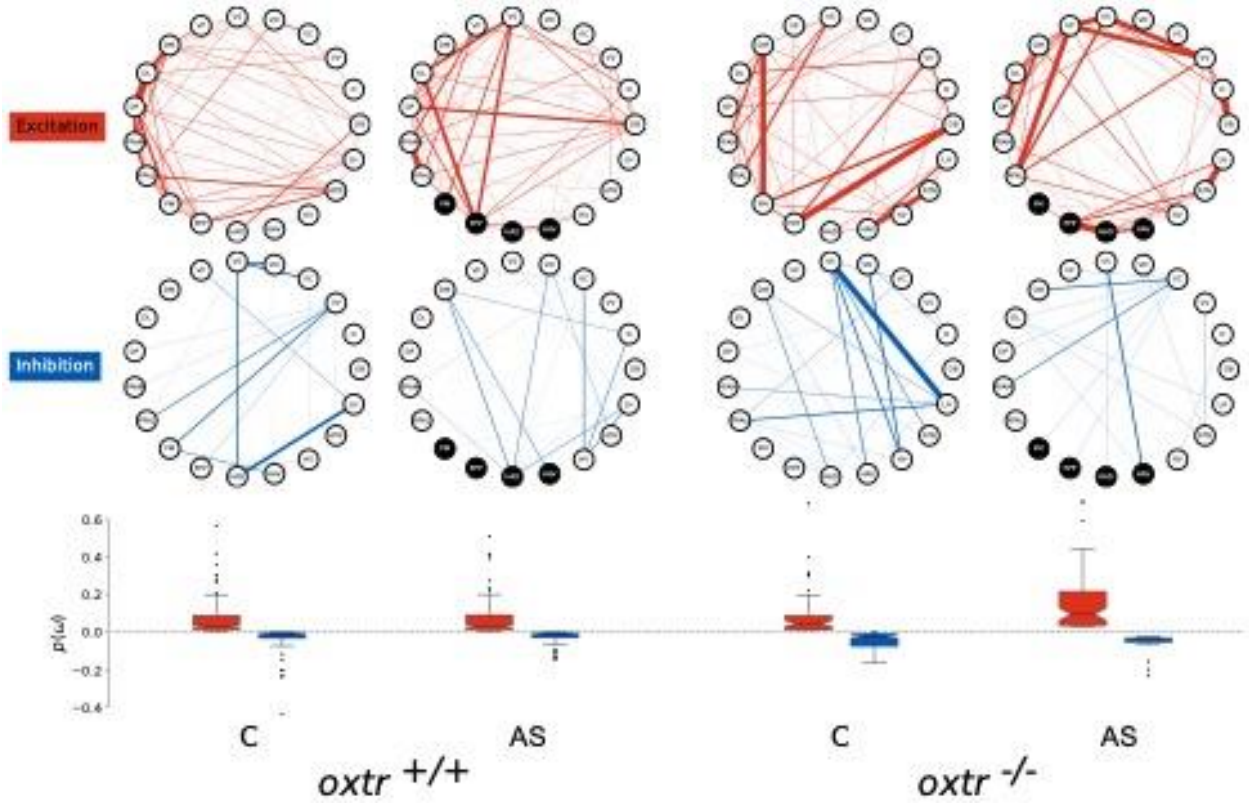

Fig. S2.

Network analysis of co-activation patterns in the social decision-making network. Nodes represent different regions and edges the relationship between them, where greater correlation values are represented by greater thickness. Networks were tested for both excitatory and inhibitory distributions across genotypes and treatments, and for computed average levels of each [probability in sample space, $p(\omega)$]. Areas of the identified preserved submodule are indicated by black nodes.

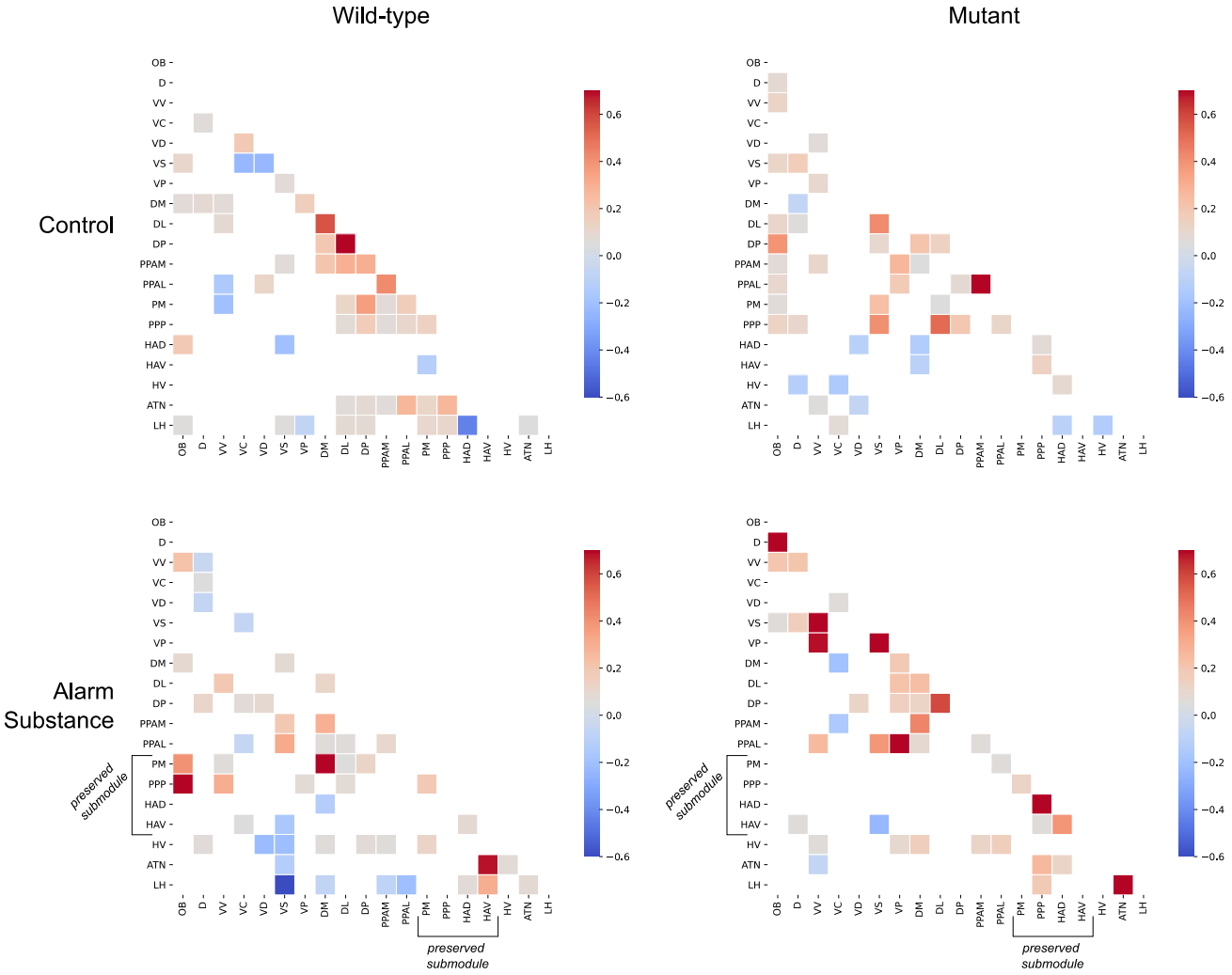

Fig. S3.

Adjacency matrices indicating inter-area connectivity. Each area's (node's) linkage with all other nodes (spearman's correlations) indicate it's centrality, which shifted with condition and genotype.

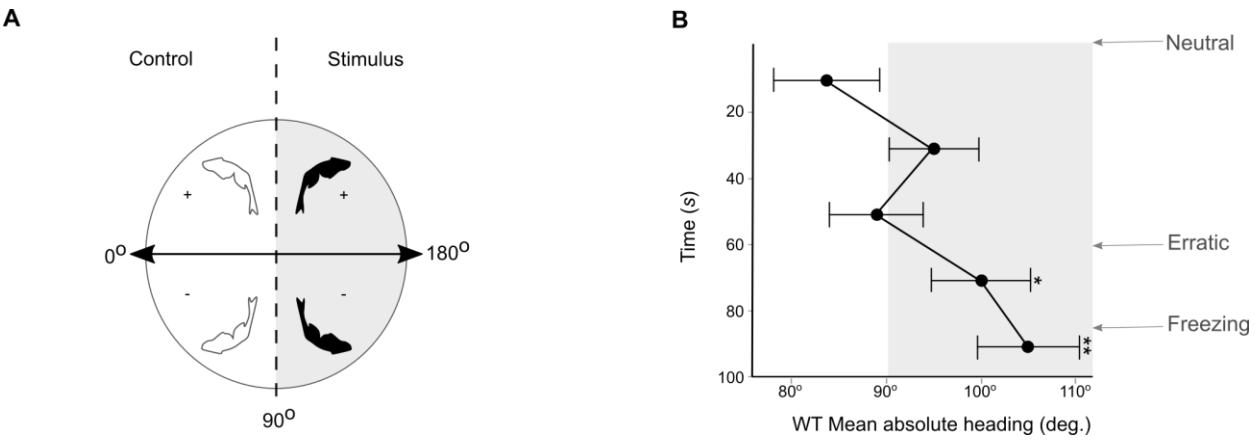

Fig. S4.

Quantification of attention towards observed neutral (control) and distress state (stimulus). (A) Absolute heading (0 - 180 degrees) towards the stimulus was used to measure distress-elicited shifts in attention. (B) Changes in attention over observation time indicate that divided attention under simultaneous presentations of neutral behaviour ($\mu > 90O$; $p > 0.05$) shifts away from neutral behavior and towards both erratic ($t\ 25 = 1.91$, $p = 0.03$) and freezing ($t\ 25 = 2.83$, $p = 0.003$) behavior when distress is demonstrated by the stimulus video.

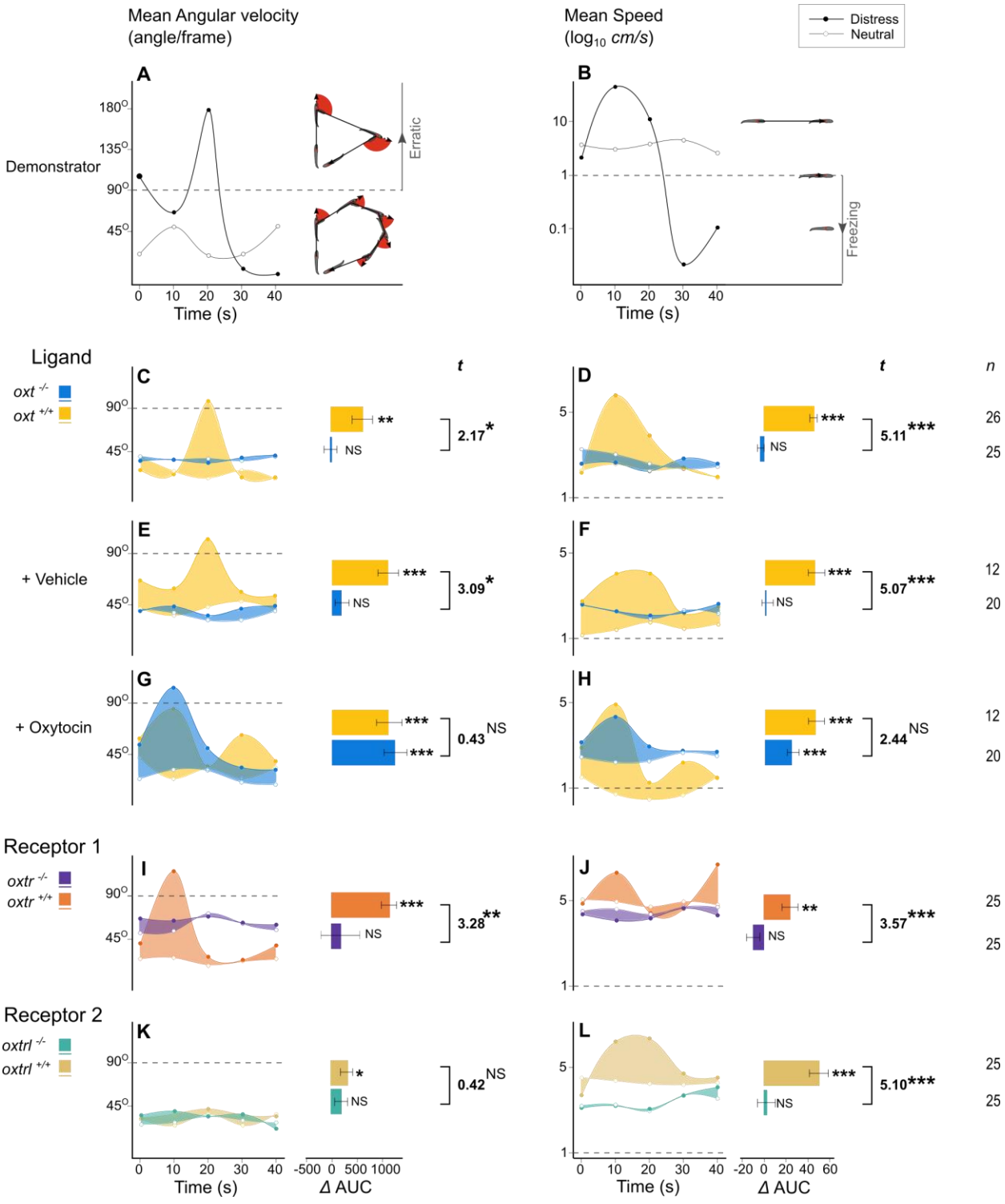

Fig. S5.

Immediate response to distress state changes. Changes from neutral to distressed behavior by the demonstrator led to: (A) increases in angular velocity with erratic movement; (B) decreases in speed during freezing. (C) Angular velocity and (D) speed changes with demonstrator shifts between neutral and stress behavior were exhibited in WT but not *oxt* KO observers. (E, F)

Genotypic effects under control treatments (vehicle), contrasted (G, H) KO fish phenotype recovery by oxytocin treatment. (I) Angular velocity increases implicated the expression of the first receptor (*oxtr*). (J) Speed changes were exhibited by WT, but not *oxtr* KO observers. (K) Expression of the second receptor (*oxtrl*) led to increases in angular velocity, but without significant differences between WT and KO observers. (L) Speed changes were significantly influenced by *oxtrl* expression. Phenotypic changes are indicated by differences in the area under the curve (Δ AUC) between neutral and stress state observations. [per-group: 1-sample t-tests, $\mu \neq 0$; between-groups: Welch's t-tests; NSP > 0.05*P < 0.05, **P < 0.01, ***P < 0.001]

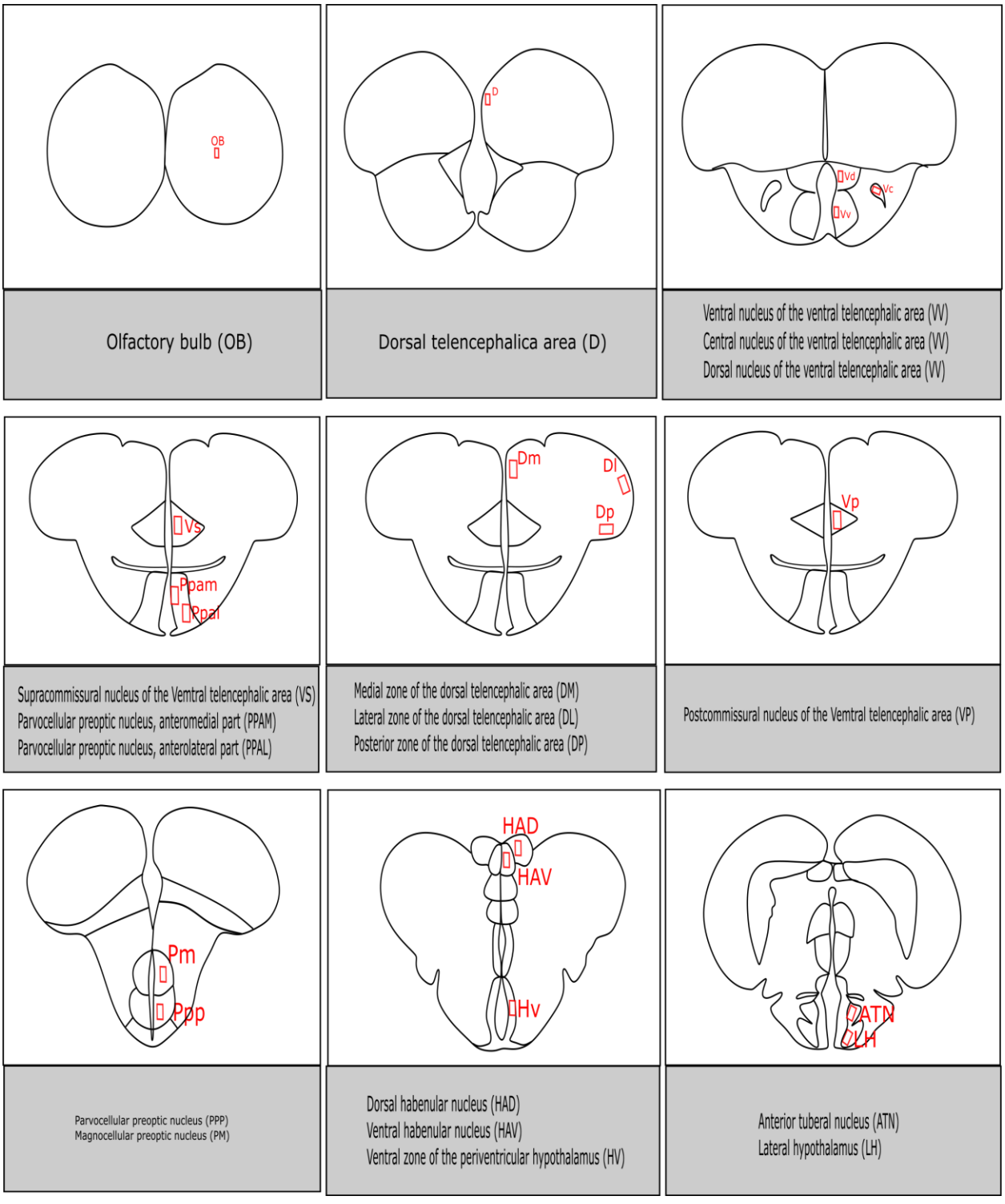

Fig. S6.

Identification of brain regions involved in social buffering of fear. The social decision-making network; a combination of the social behaviour network and the reward system *(45)*. Red rectangles represent brain regions of interest for quantifying pS6 positive cells; brain regions of interest were identified using the zebrafish brain atlas *(46)*.

Table S1.

Ranks of node strengths for each treatment for both wild-types and mutants. [Abbreviations – in brackets are mammalian homologues: OB = Olfactory bulb; VV = Ventral nucleus of ventral telencephalic area (Lateral septum); VC = Central nucleus of ventral telencephalic area (Nucleus accumbens/striatum); VD =Dorsal nucleus of ventral telencephalic area (Nucleus accumbens/striatum); VS = Supracommissural nucleus of ventral telencephalic area (Medial extended amygdala and the bed nucleus of the stria terminalis); VP = Postcommissural nucleus of ventral telencephalic area (basal amygdala); D = Dorsal telencephalic area; DM = Medial zone of dorsal telencephalic area (Medial Amygdala); DL =Lateral zone of dorsal telencephalic area (Hippocampus); DP = Posterior zone of dorsal telencephalic area (Piriform cortex); PPAM = Anterioromedial part of parvocellular preoptic nucleus (SON); PPAL = Anteriorlateral part of parvocellular preoptic nucleus (SON); PM = Magnocellular preoptic nucleus (PVN); PPP = Posterior part of parvocellular preoptic nucleus (SON); HAD = Dorsal habenular nucleus (Medial habenula); HAV = Ventral habenular nucleus (Lateral habenula); HV = Ventral zone of periventricular hypothalamus (Arcuate nucleus of the hypothalamus); ATN = Anterior tuberal nucleus (Ventromedial hypothalamus- VMH); LH = Lateral hypothalamic nucleus (Lateral hypothalamus)]

	Wild-types		**Mutants**	
	Control	**Alarm**	**Control**	**Alarm**
0	**DL**	**PPP**	**PM**	**VP**
1	**DP**	**VS**	**OB**	**VV**
2	**PPAM**	**PPAL**	**PPP**	**PPAL**
3	**DM**	**DL**	**DM**	**VS**
4	**PPAL**	**PPAM**	**HAV**	**PPP**
5	**ATN**	**DP**	**VV**	**HAD**
6	**PPP**	**OB**	**ATN**	**D**
7	**PM**	**VP**	**PPAM**	**OB**
8	**OB**	**VV**	**DL**	**ATN**
9	**VP**	**PM**	**DP**	**LH**
10	**D**	**D**	**VP**	**DM**
11	**VD**	**HAV**	**PPAL**	**DP**
12	**LH**	**ATN**	**VC**	**DL**
13	**VC**	**DM**	**D**	**HV**
14	**HV**	**VD**	**HV**	**PPAM**
15	**HAV**	**VC**	**HAD**	**HAV**
16	**VS**	**LH**	**VD**	**VD**
17	**VV**	**HAD**	**LH**	**PM**

Table S2.

Primer sequences and qRT-PCR parameters for the quantification of oxytocin receptor expression in target brain areas. (F - primer forward; R - primer reverse).

Gene	Accession No.	Primer sequence (5' → 3')	Annealing temperature (C°)	Amplicon length (pb)
eef1a1l1	NM_131263.1	F- GCTTCTCTACCTACCCTCCTCT R- CCGATTTTCTTCTCAACGCTCT	60	97
oxtr	NM_001199370.1	F-ATGAAACCTACGGCGTGAAC R-CAAGGCCAACACGGTAACTT	62	86
oxtrl	NM_001199369.1	F- TTAACGACTCCTGGGCCAAC R- CAGGGGGTTCACAGTTTGGT	60	71

Data S1. (separate file)
Spreadsheet file with all data and calculations used in this study.

References and Notes

1. F. B. de Waal, Putting the altruism back into altruism: The evolution of empathy. *Annu. Rev. Psychol.* **59**, 279–300 (2008). doi:10.1146/annurev.psych.59.103006.093625 Medline

2. F. B. M. de Waal, S. D. Preston, Mammalian empathy: Behavioural manifestations and neural basis. *Nat. Rev. Neurosci.* **18**, 498–509 (2017). doi:10.1038/nrn.2017.72 Medline

3. A. Pérez-Manrique, A. Gomila, Emotional contagion in nonhuman animals: A review. *Wiley Interdiscip. Rev. Cogn. Sci.* **13**, e1560 (2022). Medline

4. R. F. Oliveira, A. I. Faustino, Social information use in threat perception: Social buffering, contagion and facilitation of alarm responses. *Commun. Integr. Biol.* **10**, 44329 (2017). doi:10.1080/19420889.2017.1325049

5. P. F. Silva, C. G. de Leaniz, A. C. Luchiari, Fear contagion in zebrafish: A behaviour affected by familiarity. *Anim. Behav.* **153**, 95–103 (2019). doi:10.1016/j.anbehav.2019.05.004

6. J. S. Pinho, M. Castilho, J. S. Sollari, R. F. Oliveira, Innate chemical, but not visual, threat cues have been co-opted as unconditioned stimulus for social fear learning in zebrafish. *Genes Brain Behav.* **19**, e12688 (2020). doi:10.1111/gbb.12688 Medline

7. M. Davila Ross, S. Menzler, E. Zimmermann, Rapid facial mimicry in orangutan play. *Biol. Lett.* **4**, 27–30 (2008). doi:10.1098/rsbl.2007.0535 Medline

8. J. Hernandez-Lallement, P. Gómez-Sotres, M. Carrillo, Towards a unified theory of emotional contagion in rodents-A meta-analysis. *Neurosci. Biobehav. Rev.* **132**, 1229–1248 (2022). doi:10.1016/j.neubiorev.2020.09.010 Medline

9. C. Theofanopoulou, G. Gedman, J. A. Cahill, C. Boeckx, E. D. Jarvis, Universal nomenclature for oxytocin-vasotocin ligand and receptor families. *Nature* **592**, 747–755 (2021). doi:10.1038/s41586-020-03040-7 Medline

10. F. Zoratto, M. Sbriccoli, A. Martinelli, J. C. Glennon, S. Macrì, G. Laviola, Intranasal oxytocin administration promotes emotional contagion and reduces aggression in a mouse model of callousness. *Neuropharmacology* **143**, 250–267 (2018). doi:10.1016/j.neuropharm.2018.09.010 Medline

11. M. T. Pisansky, L. R. Hanson, I. I. Gottesman, J. C. Gewirtz, Oxytocin enhances observational fear in mice. *Nat. Commun.* **8**, 2102 (2017). doi:10.1038/s41467-017-02279-5 Medline

12. C. F. Zink, A. Meyer-Lindenberg, Human neuroimaging of oxytocin and vasopressin in social cognition. *Horm. Behav.* **61**, 400–409 (2012). doi:10.1016/j.yhbeh.2012.01.016 Medline

13. S. Shahrestani, A. H. Kemp, A. J. Guastella, The impact of a single administration of intranasal oxytocin on the recognition of basic emotions in humans: A meta-analysis. *Neuropsychopharmacology* **38**, 1929–1936 (2013). doi:10.1038/npp.2013.86 Medline

14. N. Speedie, R. Gerlai, Alarm substance induced behavioral responses in zebrafish (*Danio rerio*). *Behav. Brain Res.* **188**, 168–177 (2008). doi:10.1016/j.bbr.2007.10.031 Medline

15. L. A. O'Connell, H. A. Hofmann, Evolution of a vertebrate social decision-making network. *Science* **336**, 1154–1157 (2012). doi:10.1126/science.1218889 Medline

16. C. Lamm, M. Rütgen, I. C. Wagner, Imaging empathy and prosocial emotions. *Neurosci. Lett.* **693**, 49–53 (2019). doi:10.1016/j.neulet.2017.06.054 Medline

17. R. Menon, T. Grund, I. Zoicas, F. Althammer, D. Fiedler, V. Biermeier, O. J. Bosch, Y. Hiraoka, K. Nishimori, M. Eliava, V. Grinevich, I. D. Neumann, Oxytocin signaling in the lateral septum prevents social fear during lactation. *Curr. Biol.* **28**, 1066–1078.e6 (2018). doi:10.1016/j.cub.2018.02.044 Medline

18. J. Lieberz, D. Scheele, F. B. Spengler, T. Matheisen, L. Schneider, B. Stoffel-Wagner, T. M. Kinfe, R. Hurlemann, Kinetics of oxytocin effects on amygdala and striatal reactivity vary between women and men. *Neuropsychopharmacology* **45**, 1134–1140 (2020). doi:10.1038/s41386-019-0582-6 Medline

19. M. Moaddab, B. I. Hyland, C. H. Brown, Oxytocin excites nucleus accumbens shell neurons in vivo. *Mol. Cell. Neurosci.* **68**, 323–330 (2015). doi:10.1016/j.mcn.2015.08.013 Medline

20. L. S. Huffman, L. A. O'Connell, C. D. Kenkel, R. J. Kline, I. A. Khan, H. A. Hofmann, Distribution of nonapeptide systems in the forebrain of an African cichlid fish, *Astatotilapia burtoni*. *J. Chem. Neuroanat.* **44**, 86–97 (2012). doi:10.1016/j.jchemneu.2012.05.002 Medline

21. A. I. Faustino, A. Tacão-Monteiro, R. F. Oliveira, Mechanisms of social buffering of fear in zebrafish. *Sci. Rep.* **7**, 44329 (2017). doi:10.1038/srep44329 Medline

22. S. D. Preston, F. B. de Waal, Empathy: Its ultimate and proximate bases. *Behav. Brain Sci.* **25**, 1–20, discussion 20–71 (2002). doi:10.1017/S0140525X02000018 Medline

23. V. Ferretti, F. Papaleo, Understanding others: Emotion recognition in humans and other animals. *Genes Brain Behav.* **18**, e12544 (2019). Medline

24. E. G. I. Nieuwburg, A. Ploeger, M. E. Kret, Emotion recognition in nonhuman primates: How experimental research can contribute to a better understanding of underlying mechanisms. *Neurosci. Biobehav. Rev.* **123**, 24–47 (2021). doi:10.1016/j.neubiorev.2020.11.029 Medline

25. V. Ferretti, F. Maltese, G. Contarini, M. Nigro, A. Bonavia, H. Huang, V. Gigliucci, G. Morelli, D. Scheggia, F. Managò, G. Castellani, A. Lefevre, L. Cancedda, B. Chini, V. Grinevich, F. Papaleo, Oxytocin signaling in the central amygdala modulates emotion discrimination in mice. *Curr. Biol.* **29**, 1938–1953.e6 (2019). doi:10.1016/j.cub.2019.04.070 Medline

26. J. P. Burkett, E. Andari, Z. V. Johnson, D. C. Curry, F. B. de Waal, L. J. Young, Oxytocin-dependent consolation behavior in rodents. *Science* **351**, 375–378 (2016). doi:10.1126/science.aac4785 Medline

27. M. M. Rogers-Carter, J. A. Varela, K. B. Gribbons, A. F. Pierce, M. T. McGoey, M. Ritchey, J. P. Christianson, Insular cortex mediates approach and avoidance responses to social affective stimuli. *Nat. Neurosci.* **21**, 404–414 (2018). doi:10.1038/s41593-018-0071-y Medline

28. L. F. Li, W. Yuan, Z. X. He, L. M. Wang, X. Y. Jing, J. Zhang, Y. Yang, Q. Q. Guo, X. N. Zhang, W. Q. Cai, W. J. Hou, R. Jia, F. D. Tai, Involvement of oxytocin and GABA in consolation behavior elicited by socially defeated individuals in mandarin

voles. *Psychoneuroendocrinology* **103**, 14–24 (2019). doi:10.1016/j.psyneuen.2018.12.238 Medline

29. A. Yamagishi, J. Lee, N. Sato, Oxytocin in the anterior cingulate cortex is involved in helping behaviour. *Behav. Brain Res.* **393**, 112790 (2020). doi:10.1016/j.bbr.2020.112790 Medline

30. S. W. Chang, J. W. Barter, R. B. Ebitz, K. K. Watson, M. L. Platt, Inhaled oxytocin amplifies both vicarious reinforcement and self reinforcement in rhesus macaques (*Macaca mulatta*). *Proc. Natl. Acad. Sci. U.S.A.* **109**, 959–964 (2012). doi:10.1073/pnas.1114621109 Medline

31. N. Percie du Sert, V. Hurst, A. Ahluwalia, S. Alam, M. T. Avey, M. Baker, W. J. Browne, A. Clark, I. C. Cuthill, U. Dirnagl, M. Emerson, P. Garner, S. T. Holgate, D. W. Howells, N. A. Karp, S. E. Lazic, K. Lidster, C. J. MacCallum, M. Macleod, E. J. Pearl, O. H. Petersen, F. Rawle, P. Reynolds, K. Rooney, E. S. Sena, S. D. Silberberg, T. Steckler, H. Würbel, The ARRIVE guidelines 2.0: Updated guidelines for reporting animal research. *J. Cereb. Blood Flow Metab.* **40**, 1769–1777 (2020). doi:10.1177/0271678X20943823 Medline

32. L. Thomas, F. Juanes, The importance of statistical power analysis: An example from Animal Behaviour. *Anim. Behav.* **52**, 856–859 (1996). doi:10.1006/anbe.1996.0232

33. D. Szucs, J. P. Ioannidis, Empirical assessment of published effect sizes and power in the recent cognitive neuroscience and psychology literature. *PLOS Biol.* **15**, e2000797 (2017). doi:10.1371/journal.pbio.2000797 Medline

34. A. C. Borges, N. Pereira, M. Franco, L. Vale, M. Pereira, M. V. Cunha, A. Amaro, T. Albuquerque, M. Rebelo, Implementation of a zebrafish health program in a research facility: A 4-year retrospective study. *Zebrafish* **13** (Suppl 1), S115–S126 (2016). doi:10.1089/zeb.2015.1230 Medline

35. J. Blechman, S. Anbalagan, G. G. Matthews, G. Levkowitz, Genome editing reveals idiosyncrasy of CNGA2 ion channel-directed antibody immunoreactivity toward oxytocin. *Front. Cell Dev. Biol.* **6**, 117 (2018). doi:10.3389/fcell.2018.00117 Medline

36. A. R. Nunes, L. Carreira, S. Anbalagan, J. Blechman, G. Levkowitz, R. F. Oliveira, Perceptual mechanisms of social affiliation in zebrafish. *Sci. Rep.* **10**, 3642 (2020). doi:10.1038/s41598-020-60154-8 Medline

37. D. Braida, A. Donzelli, R. Martucci, V. Capurro, M. Busnelli, B. Chini, M. Sala, Neurohypophyseal hormones manipulation modulate social and anxiety-related behavior in zebrafish. *Psychopharmacology* **220**, 319–330 (2012). doi:10.1007/s00213-011-2482-2 Medline

38. R. B. D'Agostino, in *Goodness-of-Fit Techniques*. R. B. D'Agostino, M. A. Stephens, Eds., (Marcel Dekker, 1986), pp. 97-193.

39. K. J. Livak, T. D. Schmittgen, Analysis of relative gene expression data using real-time quantitative PCR and the 2(-Δ Δ C(T)) Method. *Methods* **25**, 402–408 (2001). doi:10.1006/meth.2001.1262 Medline

40. J. X. Goh, J. A. Hall, R. Rosenthal, Mini meta-analysis of your own studies: Some arguments on why and a primer on how. *Soc. Personal. Psychol. Compass* **10**, 535–549 (2016). doi:10.1111/spc3.12267

41. D. Chawla, A. Deorari, Inferential statistics: Introduction to hypothesis testing. *J. Neonatol.* **19**, 259–264 (2005). doi:10.1177/0973217920050313

42. F. De Vico Fallani, V. Latora, M. Chavez, A topological criterion for filtering information in complex brain networks. *PLOS Comput. Biol.* **13**, e1005305 (2017). doi:10.1371/journal.pcbi.1005305 Medline

43. V. A. Traag, J. Bruggeman, Community detection in networks with positive and negative links. *Phys. Rev. E Stat. Nonlin. Soft Matter Phys.* **80**, 036115 (2009). doi:10.1103/PhysRevE.80.036115 Medline

44. T. P. Peixoto, Revealing consensus and dissensus between network partitions. *Phys. Rev. X* **11**, 021003 (2021). doi:10.1103/PhysRevX.11.021003

45. L. A. O'Connell, H. A. Hofmann, The vertebrate mesolimbic reward system and social behavior network: A comparative synthesis. *J. Comp. Neurol.* **519**, 3599–3639 (2011). doi:10.1002/cne.22735 Medline

46. M. F. Wullimann, B. Rupp, H. Reichert, *Neuroanatomy of the Zebrafish Brain: A Topological Atlas* (Springer, 1996).